

High resolution numerical modeling of the force-free pulsar magnetosphere

Andrey Timokhin

Sternberg Astronomical Institute, Moscow, Russia

December 9, 2018

Abstract

We consider the force-free magnetosphere of an aligned rotator. Its structure is well described by a Grad-Shafranov equation for poloidal magnetic field, the so-called "pulsar equation". We solve this equation by a multigrid method with high numerical resolution. On the fine numerical grid current layer along the last closed field line could be accurately incorporated into the numerical procedure and all physical properties of the solution such as Goldreich-Julian charge density, drift velocity, energy losses etc. could be accurately calculated. Here we report results of the simulations. Among other interesting properties, the solution is not unique, i.e. the position of the last closed field line, and hence the pulsar energy losses, are not determined by the global magnetosphere structure and depend on kinetic of electromagnetic cascades. We discuss the properties of the solutions and their implications for pulsars. A model for pulsar magnetosphere evolution is proposed. In the frame of this model values of the pulsar braking index less than 3 have natural explanation.

1 Pulsar Equation

We consider the force-free magnetosphere of an aligned rotator. Such magnetosphere is well described by the so-called pulsar equation (Michel, 1973; Scharlemann & Wagoner, 1973; Okamoto, 1974). For young pulsars the differential rotation of the open field lines could be neglected and the pulsar equation takes the form (see e.g. Goodwin et al., 2004)

$$(x^2 - 1)(\partial_{xx}\psi + \partial_{zz}\psi) + \frac{x^2 + 1}{x}\partial_x\psi - S\frac{dS}{d\psi} = 0 \quad (1)$$

All coordinates are normalized to the light cylinder radius $R_{LC} \equiv c/\Omega$. We use normalization for ψ , where the dipole magnetic field function near the NS surface is given by

$$\psi^{\text{dip}} = \frac{x^2}{(x^2 + z^2)^{3/2}}, \quad (2)$$

The normalized poloidal current function S is given by $S \equiv (4\pi/c)(R_{\text{LC}}^2/\mu)I$, where $\mu \equiv B_0 R_{\text{NS}}^3/2$ is the magnetic momentum of the NS. Magnetic field is expressed through the functions I and $\Psi \equiv (\mu/R_{\text{LC}})\psi$ as

$$\mathbf{B} = \frac{\nabla\Psi \times \mathbf{e}_\phi}{\varpi} + \frac{4\pi}{c} \frac{I}{\varpi} \mathbf{e}_\phi \quad (3)$$

The poloidal current S is found from the condition at the light cylinder

$$\partial_x \psi|_{\text{LC}} = \frac{1}{2} SS'|_{\text{LC}} \quad (4)$$

We assume existence of an equatorial current sheet with the return current. The equatorial current sheet can be excluded from the numerical treatment by setting appropriate boundary conditions at the equatorial plane. For the current sheet at the boundary between closed and open field line regions this is not possible, and we smear the return current flowing along the last closed magnetic field line over the region $[\psi_{\text{last}} - d\psi, \psi_{\text{last}}]$, see Fig. 1.

A solution of the pulsar equation (1) for dipolar magnetic field geometry had been found for the first time by Contopoulos et al. (1999). They assumed, that the last closed field line is fixed at the light cylinder. Later Goodwin et al. (2004) have found solutions for different positions x_0 of the point, where the last closed field line intersects the equatorial plane, inside the light cylinder, $x_0 \leq 1$. However they have made a rather unnatural assumption, that the plasma pressure inside the closed field line domain is finite and plays an important role in the force balance across magnetic field lines.

We perform calculations for different $x_0 \leq 1$ with high numerical resolution using grids with number of points in each directions ranging from 2000 to 6000. In contrast to Goodwin et al. (2004) we assume zero pressure inside the closed field line region, i.e. the plasma there is cold. Equation (1) is solved numerically in the domain $x_{\text{NS}} \leq x \leq x_{\text{max}}, z_{\text{NS}} \leq z \leq z_{\text{max}}$. Boundary conditions are shown in Fig. 1. The equation (1) is solved by a full multigrid (V-cycles) FAS scheme (see Trottenberg et al., 2001). We use Gauss-Seidel smoother and SOR Gauss-Seidel solver at the coarsest level. Independence of the obtained results on the domain sizes $(x_{\text{NS}}, x_{\text{max}}, z_{\text{NS}}, z_{\text{max}})$, $d\psi$ and algorithm-specific parameters has been verified.

We have expanded ψ at the light cylinder in the Taylor series up to the second order terms, and substituted this expansion into the pulsar equation imposing the continuity of ψ at the light cylinder. In this way we obtained an equation for ψ at the light cylinder, accurate up to the second order term, what is sufficient for our numerical treatment, because we use a second order scheme. Eq.(4) is used for determination of the poloidal current. Such techniques was used by Goodwin et al. (2004) in their simulations. It allows numerical treatment of the problem in a single domain, rather than doing extremely CPU time consuming matching of the solutions inside an outside the light cylinder, as it was made by Contopoulos et al. (1999).

2 Main Results

- Calculations have been performed for the following values of x_0 : 0.15; 0.2; 0.3; 0.4; 0.5; 0.6; 0.7; 0.8; 0.9; 0.95; 0.992. An unique solution has been found for each of the above x_0 's. As representative examples, in Figs. 3-8 properties of solutions for three cases ($x_0 = 0.2; 0.7; 0.99$) are shown.
- Each solution has been checked for applicability of the force-free condition $E < B$. In none of them this condition is violated, at least up to 16 light cylinder radii from the NS. The force-free condition can be reformulated as the condition on the drift velocity

$$\mathbf{u}_D = \frac{1}{c} \frac{\mathbf{E} \times \mathbf{B}}{B^2} < c. \quad (5)$$

In Figs. 3,5,7 maps of u_D for three values of x_0 : 0.2, 0.6 and .99, are shown. One can see, that the critical value of $u_D = 1$ is never achieved. In all other cases the situation is similar.

- For x_0 close to 1 ($x_0 = 0.95; 0.99; 0.992$) the magnetic field strength B at the equatorial plane increases very rapidly when x approaches x_0 . The maximum value of B , achieved in the closed field line domain near the point x_0 , increases with increasing of x_0 and decreasing of $d\psi$, see Fig. 1. We interpret this as a result of $\lim_{x \rightarrow 1} B = \infty$, predicted by Gruzinov (2005).
- Energy losses of the pulsar for each x_0 have been calculated numerically. They increase with decreasing of x_0 and can be described by the formula

$$W = A(x_0) * W_{md} \equiv A(x_0) * \frac{2}{3} \frac{\mu^2 \Omega^4}{c^3}, \quad (6)$$

where W_{md} are magnetodipolar energy losses. The function $A(x_0)$ can be fitted surprisingly well by the power law

$$A(x_0) = 1.41 x_0^{-2.065}, \quad (7)$$

see Fig. 10. We note, that analytical estimations of the energy losses based on the Michel poloidal current distribution for the dipolar magnetic field gives

$$A(x_0) = x_0^{-2} \quad (8)$$

- The total energy of the electromagnetic field in the magnetosphere $E_{tot} = \int \frac{B^2 + E^2}{8\pi} dV$ decreases with increasing of x_0 , see Fig. 10.
- In configurations with $x_0 > 0.6$ there is a *volume* return current flowing along the open magnetic field lines, which carries however only a small part of the whole return current. For $x_0 \leq 0.6$ the return current flows only along the last open field line. On Fig.11 the volume current density

along open field lines in the polar cap of pulsar is shown. One can see, that the current density (in units of j_{GJ}) close to the polar cap boundary increases with increasing of x_0 . The current density does not exceed the Goldreich-Julian current density $j_{GJ} \equiv \rho_{GJ}c$ and at most field lines it is *less* than j_{GJ} .

3 Evolution of the pulsar magnetosphere

For each x_0 a special unique volume current distribution is necessary in order to support a force-free configuration of the magnetosphere. The current density along open field lines in the polar cap of pulsar could adjust to the values required by the global magnetosphere structure (both smaller and greater than j_{GJ}) when there is a particle *inflow* from the magnetosphere into the polar cap acceleration zone (Lyubarskij, 1992). As a source of particles in the magnetosphere the outer gap cascade could be considered. On the other hand, when the polar cap cascade is strong and produces a lot of secondary particles with a wide energy distribution, some of these particles with the smallest energies, can be reversed in the outer magnetosphere either as a result of momentum redistribution in the turbulent outflowing plasma, or by a weak electric field arising as the magnetosphere will try to achieve the most energetically favorably, i.e. force-free, configuration. The polar cap and the outer gap cascades can not supply any arbitrary particle density, and, hence, can not support any arbitrary current density in the magnetosphere. However, a current with density greater or smaller than j_{GJ} can flow through the polar cap acceleration zone only if there is a particle inflow from the magnetosphere. The larger the deviation of j from j_{GJ} , the larger particle flux from the magnetosphere is necessary. So, when the pulsar becomes older, the range of current densities, which could be supported by the cascades becomes smaller and the magnetosphere should change configuration to a new one, where the required current density could be supported by the weaker cascades.

As the electromagnetic energy of the magnetosphere decreases with increasing of x_0 , the most preferably configuration is that, where the null point (point where the last closed field line intersects the equatorial plane) lies at the light cylinder. However, in such configuration the deviation of the poloidal current density at the open field lines from the Goldreich-Julian current density is the largest and, hence, this requires a powerful source of the particles in the magnetosphere. When the pulsar becomes older and cannot support such poloidal current, the null point moves to a new position, closer to the NS, corresponding to a magnetosphere configuration, where the deviation of the current density from j_{GJ} is smaller and such current density could be supported by the weaker cascades. In the new configuration the energy losses (for the same Ω) are larger than in the configuration with $x_0 = 1$ and, hence, the energy losses of pulsar decrease with time slower than it is given by the magnetodipolar formula. If at some time the dependence of x_0 on the pulsar age and, hence, on Ω is given by

$x_0 \propto \Omega^\xi$, then using eqs. (7),(6) we get

$$W \propto \Omega^\alpha, \quad \alpha = 4 - 2.065 \xi, \quad (9)$$

ξ is a complicated function of the pulsar age t , but as x_0 decreases with t (see above), it is always positive, $\xi(t) > 0$. So, the braking index

$$n = \frac{\ddot{\Omega}\Omega}{\dot{\Omega}^2} = \alpha - 1 = 3 - 2.065 \xi, \quad (10)$$

is always less than 3!

Detailed description of the numerical method and results of calculation, as well as discussion of their implication for pulsar physics, are given in Timokhin (2005).

This work was supported by RFBR grant 04-02-16720.

References

- Contopoulos I., Kazanas D., Fendt C., 1999, ApJ, 511, 351
- Goodwin S. P., Mestel J., Mestel L., Wright G. A. E., 2004, MNRAS, 349, 213
- Gruzinov A., 2005, Phys.Rev.Lett., 94, 021101
- Lyubarskij Y. E., 1992, A&A, 261, 544
- Michel F. C., 1973, ApJ Letters, 180, L133
- Okamoto I., 1974, MNRAS, 167, 457
- Scharlemann E. T., Wagoner R. V., 1973, ApJ, 182, 951
- Timokhin A. N., 2005, in preparation
- Trottenberg U., Oosterlee C. W., Schüller A., Brandt A., Oswald P., Stüben K., 2001, Multigrid. Academic Press

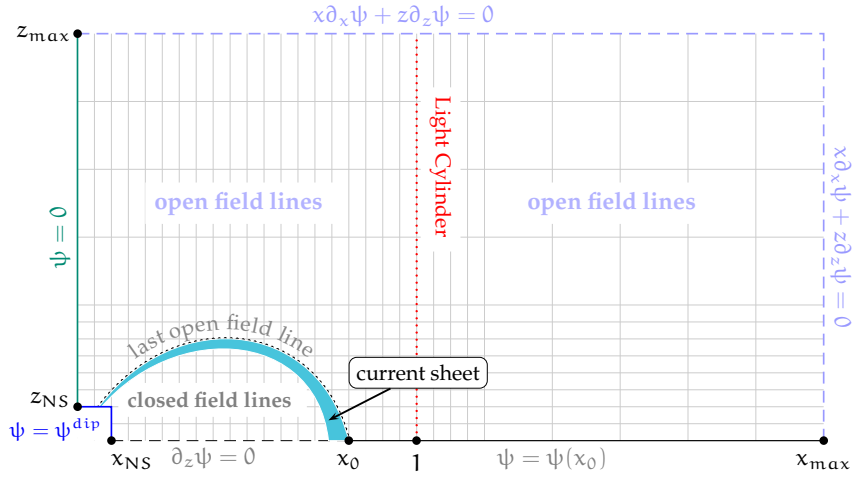


Figure 1: Calculation domain and boundary conditions

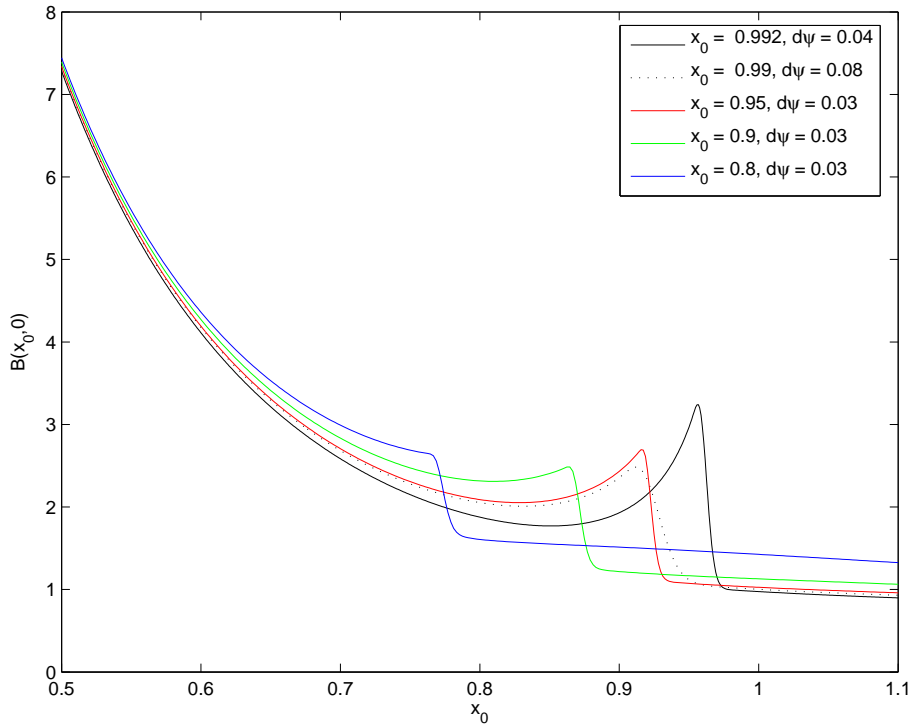


Figure 2: Magnetic field strength at the equatorial plane as a function of x for different x_0 and widths of the current sheet.

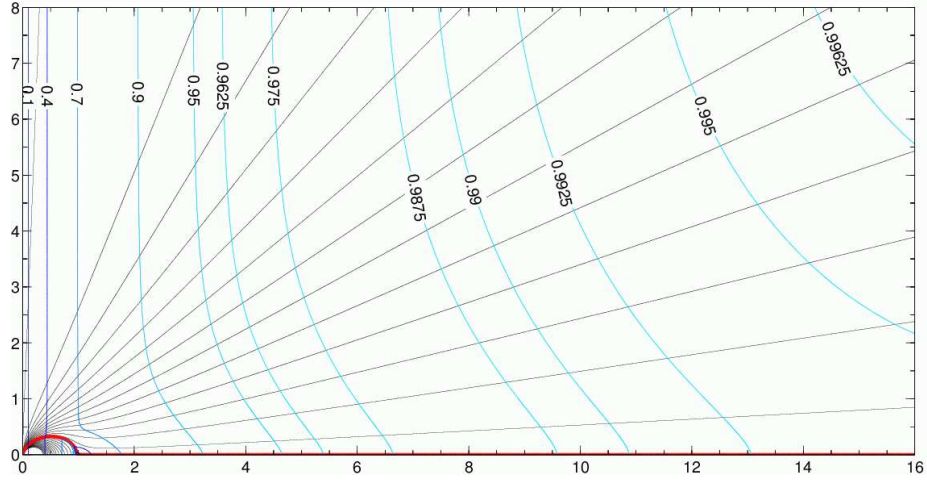


Figure 3: Magnetic field lines configuration (radial black lines) for $x_0 = 0.99$, $d\psi = 0.08$. The last closed field line is shown by the thick red line. Contours of the absolute values of the drift velocity normalized to the speed of light, $|\mathbf{u}_D|/c$, are shown by the blue vertical lines.

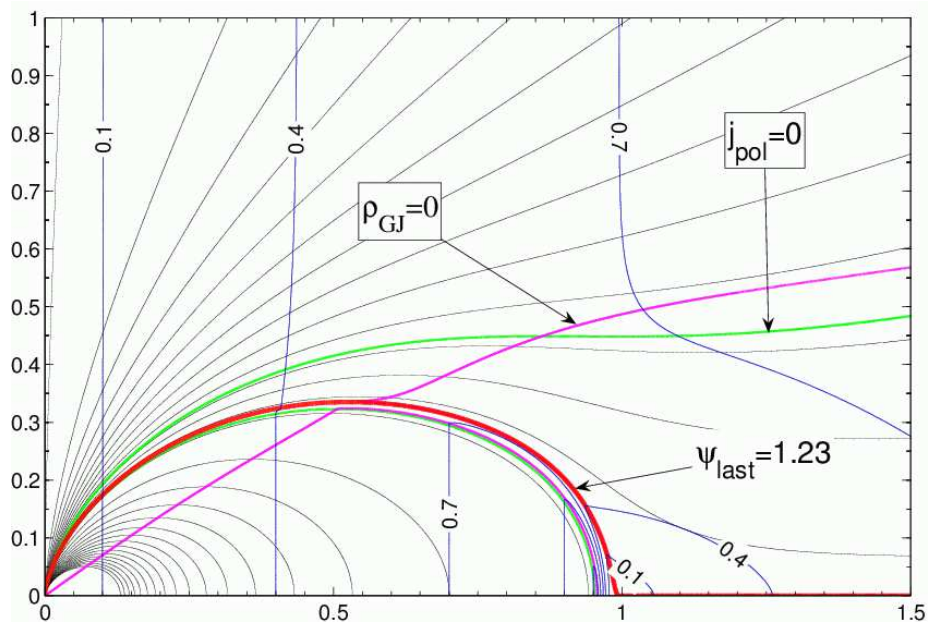


Figure 4: Central parts of the magnetosphere for $x_0 = 0.992$, $d\psi = 0.04$. Notations similar to ones in Fig. 3. Also line where ρ_{GJ} changes sign and $j_{pol} = 0$ are shown.

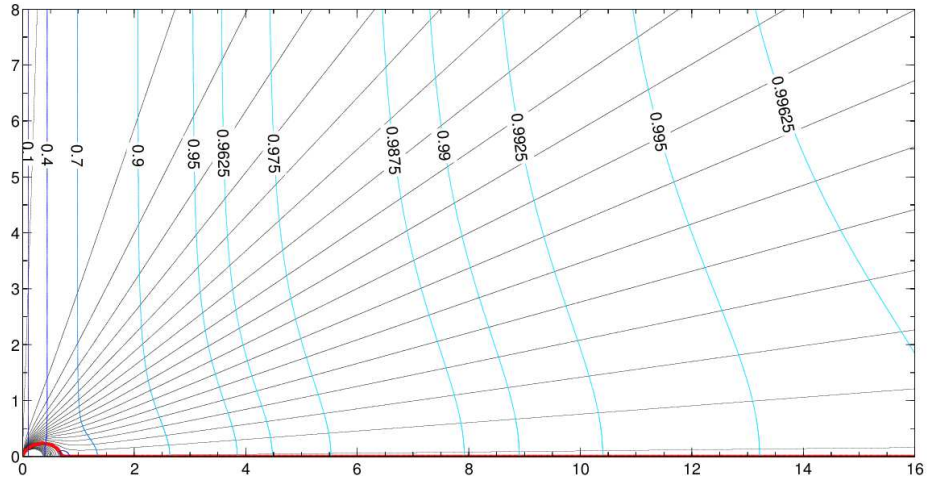


Figure 5: Drift velocity and magnetic field configuration for $x_0 = 0.7$, $d\psi = 0.03$

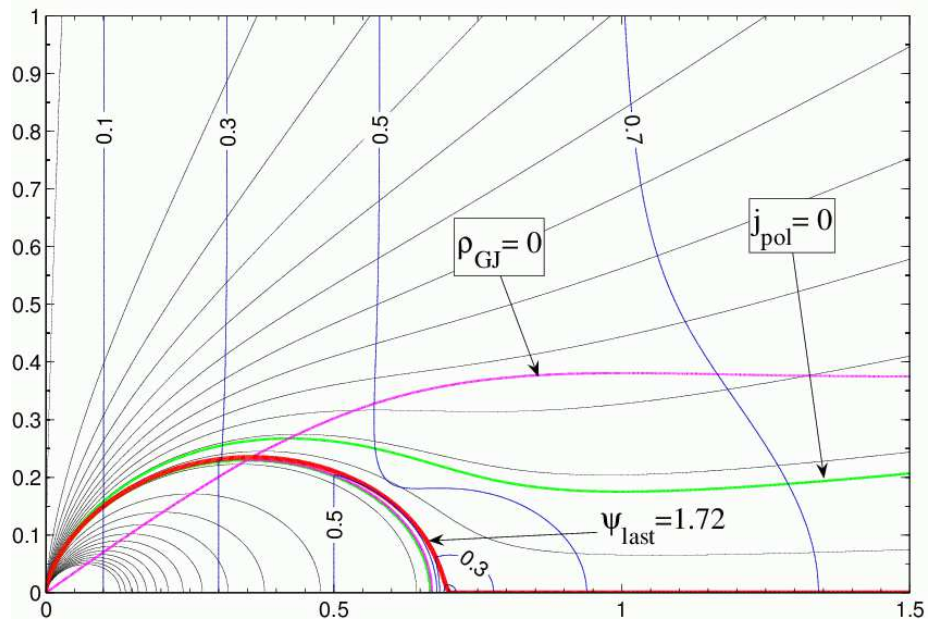


Figure 6: Inner parts of Fig. 5.

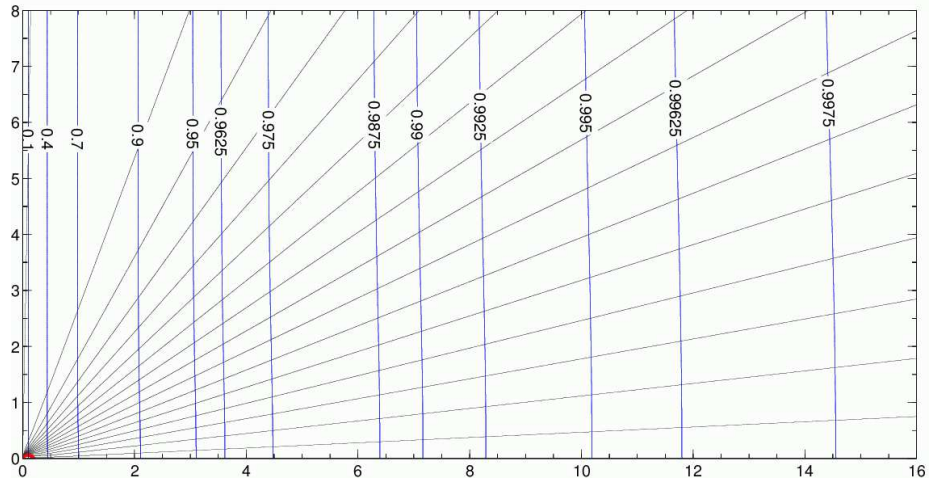


Figure 7: Drift velocity and magnetic field configuration for $x_0 = 0.2, d\psi = 0.03$

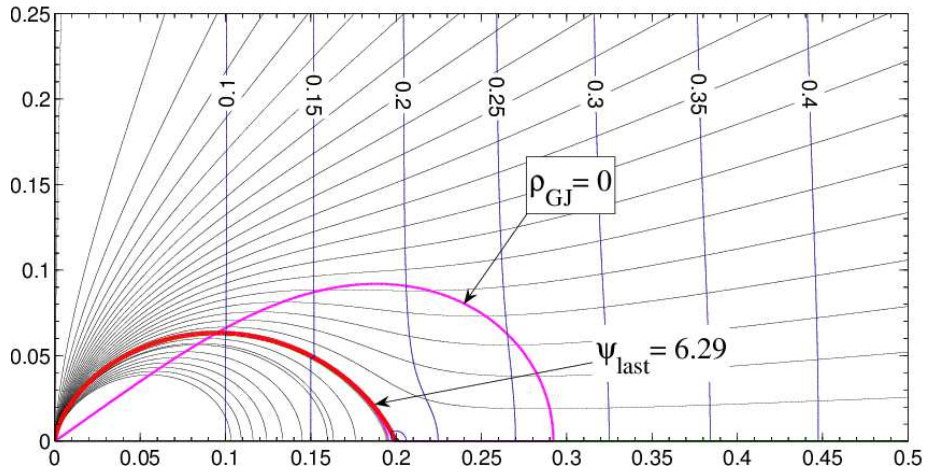


Figure 8: Inner parts of Fig. 7.

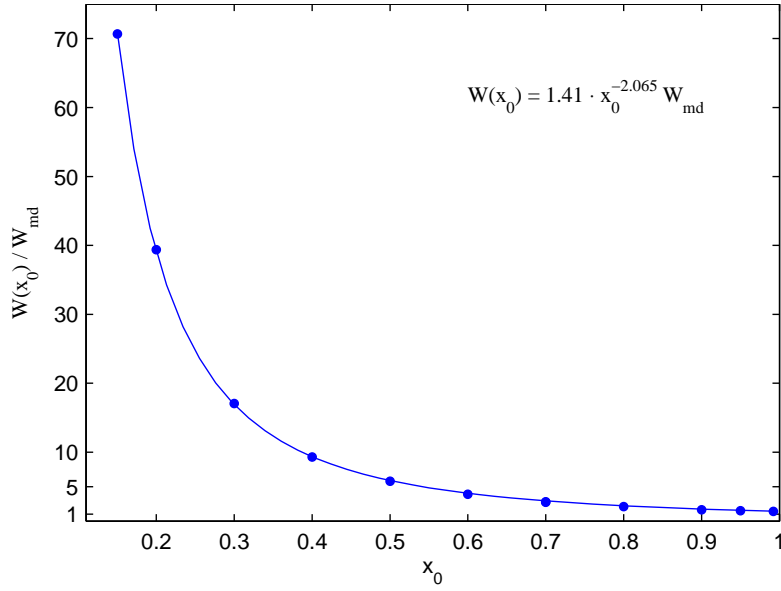


Figure 9: Numerically calculated energy losses normalized to the magnetodipolar energy losses as a function of x_0 (dots). Fit of the results by the power law is shown by the solid blue line.

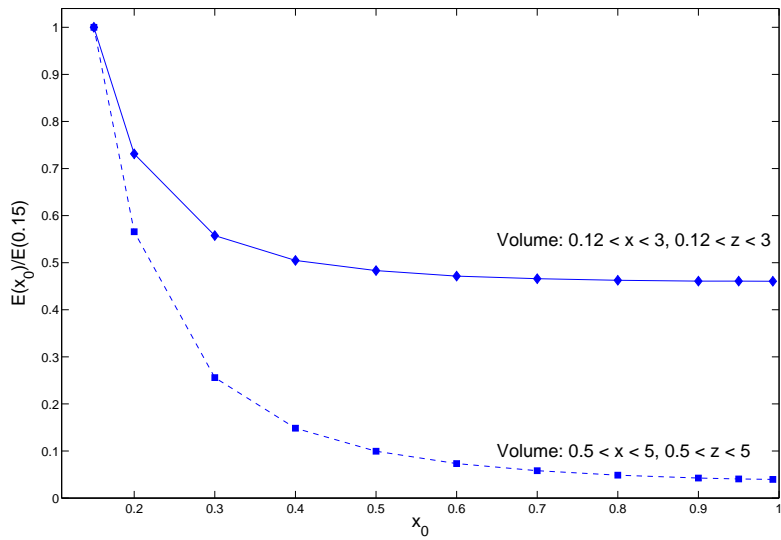


Figure 10: Total electromagnetic energy of two different volumes as a function of x_0 . The values were normalized to the energy in the corresponding volumes for $x_0 = 0.15$.

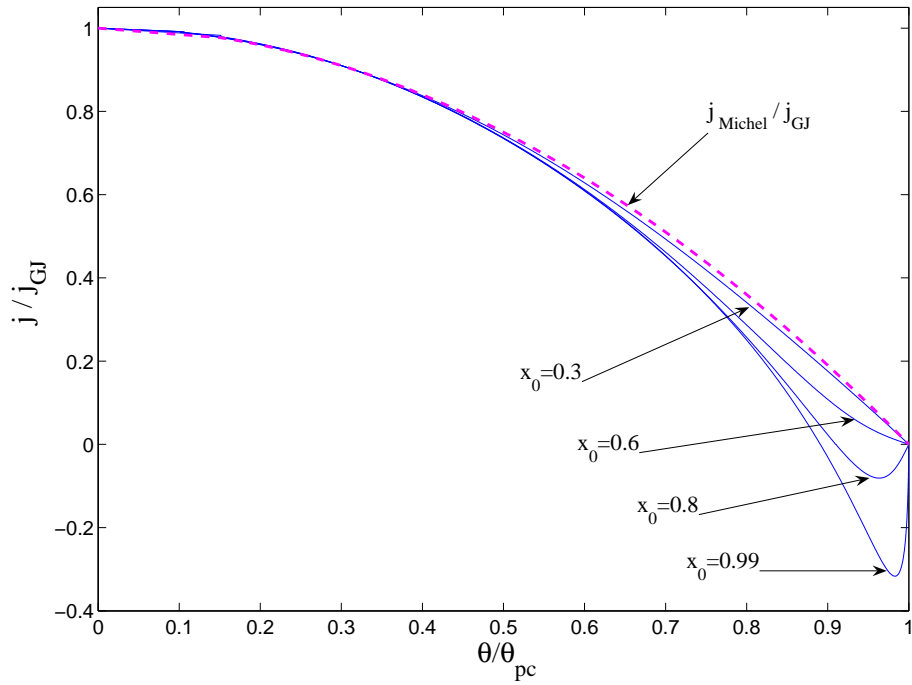


Figure 11: Poloidal current density in the polar cap of pulsar for different values of x_0 , normalized to the corresponding Goldreich-Julian current density as a function of the colatitude, normalized to the colatitude of the polar cap boundary θ_{pc} . Michel current density is shown by the dashed line